Controlled modification of mono- and bilayer graphene in O, H and CF plasmas

Felten, A.; Pireaux, J.-J.; Eckmann, A.; Casiraghi, C.; Krupke, R.

Published in:
Nanotechnology

DOI:
10.1088/0957-4484/24/35/355705

Publication date:
2013

Document Version
Publisher's PDF, also known as Version of record

Controlled modification of mono- and bilayer graphene in O_2, H_2 and CF_4 plasmas

2013 Nanotechnology 24 355705

(http://iopscience.iop.org/0957-4484/24/35/355705)

Nanotechnology **24** (2013) 355705 (8pp) doi:10.1088/0957-4484/24/35/355705

Controlled modification of mono- and bilayer graphene in O_2, H_2 and CF_4 plasmas

A Felten[1], A Eckmann[2], J-J Pireaux[1], R Krupke[3,4] and C Casiraghi[2,5]

[1] Research Center in Physics of Matter and Radiation (PMR), University of Namur, B-5000 Namur, Belgium
[2] School of Chemistry, University of Manchester, Manchester M13 9PL, UK
[3] Institute of Nanotechnology, Karlsruhe Institute of Technology, D-76021 Karlsruhe, Germany
[4] Department of Materials and Earth Sciences, Technische Universität Darmstadt, D-64287 Darmstadt, Germany
[5] Physics Department, Free University Berlin, Arnimallee 14, D-14195 Berlin, Germany

E-mail: alexandre.felten@unamur.be

Received 14 May 2013, in final form 26 June 2013
Published 12 August 2013
Online at stacks.iop.org/Nano/24/355705

Abstract
In this work, covalent modification of mono- and bilayer graphene is achieved using tetrafluoromethane (CF_4), oxygen and hydrogen RF plasma. Controlled modification of graphene is usually difficult to achieve, in particular with oxygen plasma, which is rather aggressive and usually leads to etching of graphene. Here we use x-ray photoelectron spectroscopy and Raman spectroscopy to show that mild plasma conditions and fine tuning of the number of functional groups can be obtained in all plasmas by varying parameters such as exposure time and sample position inside the chamber. We found that even for the usual harsh oxygen treatment the defect density could be lowered, down to one defect for 3.5×10^4 carbon atoms. Furthermore, we show that CF_4 plasma leads to functionalization without etching and that graphene becomes an insulator at saturation coverage. In addition, the reactivity of mono- and bilayer graphene was studied revealing faster modification of monolayer in oxygen and CF_4 plasma, in agreement with previous works. In contrast, similar modification rates were observed for both mono- and bilayer during hydrogenation. We attribute this discrepancy to the presence of more energetic species in the hydrogen plasma such as positive ions that could play a role in the functionalization process.

S Online supplementary data available from stacks.iop.org/Nano/24/355705/mmedia

(Some figures may appear in colour only in the online journal)

1. Introduction

Despite its unique structural and electronic properties [1, 2], graphene suffers from several drawbacks which slow down the route towards applications. For instance, the absence of a gap in the band structure and its chemical inertness are among the most serious issues [3]. In order to overcome such problems, various approaches to tune and to control the chemical and electronic properties of graphene have been considered. In this work, we focus more specifically on the chemical modification of graphene through plasma treatments. Increasing interest in this technique has been shown lately because of its advantages over other chemical processes. The plasma treatment is a simple, fast and scalable process. Furthermore, it can be easily implemented in the electronic device production line and a large variety of functional groups can be attached to the graphene surface. For example, oxygen [4–6], hydrogen [7–9], nitrogen [10–12], fluorine [13–15], chlorine [16] or boron [17] were successfully attached to the carbon lattice using this technique. The chemisorptions of these atoms transform the sp^2 carbon hybridization into sp^3 and can lead to

new graphene-based derivatives, such as graphane and fluoro-graphene [18, 19], with a theoretically predicted band gap between 3 and 6 eV [6, 20, 21].

One of the main concerns in graphene functionalization is to have a precise control on the number and type of functional groups attached to the graphene surface, which would allow fine tuning of the electronic properties of graphene from metallic to insulating. Hydrogen or fluorine plasma treatments have been shown to induce rather controllable modification [14, 15]. However the specific results vary from one study to another. For example, Wu *et al* [16] evidenced rapid destruction of graphene using hydrogen plasma contrary to other studies [18, 7]. Furthermore, Jaiswal *et al* [9] have shown similar modification rates for both mono- and bilayer graphene in hydrogen plasma, while Luo *et al* [8] observed that hydrogenation of single-layer graphene is much less feasible than that of bilayer graphene. This indicates the complexity of such treatments and the importance of taking into account the experimental setup, i.e. capacitive or inductive coupling, RF or microwave, etc. Oxygen plasma, on the other hand, being very aggressive, usually results in quick and drastic changes of the structural and electronic properties of graphene: a high degree of disorder is induced in the graphene lattice even at low power and after a very short exposure time [22, 6]. Thus, despite its high potential, plasma treatment of graphene needs further investigation in order to fully understand the effect of the experimental parameters on the specific modification of graphene.

In this work, we investigated the modification of mono- and bilayer graphene using oxygen (O_2), hydrogen (H_2) and tetrafluoromethane (CF_4) plasma treatments. All experiments have been carried out in the same plasma system in order to allow direct comparison of the results. Chemical functionalization is confirmed by x-ray photoelectron spectroscopy (XPS) measurements on exfoliated modified monolayer graphene. Structural changes have been monitored by Raman spectroscopy. In contrast to other studies, we show that highly controllable modification can be achieved in all types of plasma, by varying different parameters such as exposure time and sample position inside the chamber. Furthermore, we compared fluorination, oxygenation and hydrogenation of a single-layer and a bilayer. We show that graphene is more reactive than a bilayer for fluorination and oxygenation, while hydrogen plasma leads to a similar modification rate for both mono and bilayer graphene. We attribute this difference to the presence of more energetic species in the hydrogen plasma such as positive ions that could reach the graphene surface and play an important role in the functionalization process. Our results provide useful information to obtain a highly controlled chemical functionalization of graphene using plasma processes, a flexible tool that could be easily implemented in the fabrication of graphene-based devices.

2. Experimental methods

Graphene was mechanically exfoliated onto 300 nm grown silicon oxide on a doped silicon substrate. Graphene sheets were identified by optical microscopy and the number of layers was confirmed using Raman spectroscopy. The graphene sheets were modified in a home-made chamber using inductively coupled plasma at RF of 13.56 MHz described elsewhere [23]. The plasma treatments were performed at a power of 10 W and a pressure of 0.1 Torr. The power was kept at low value to avoid rapid damaging of the graphene while still allowing quick ignition of the plasma. The treatment duration was varied between 2 and 300 s. Two positions inside the chamber were chosen for the sample: one inside the glow discharge (referred to as position 1) and another in the afterglow discharge (30 cm away from the center of the discharge, referred to as position 2). Figure S1 (in SI available at stacks.iop.org/Nano/24/355705/mmedia) shows the scheme of the plasma chamber with the exact positions of the samples. Oxygen, hydrogen or tetrafluoromethane was introduced inside the chamber in order to partially oxidize, hydrogenate or fluorinate the graphene, respectively.

Grafting of chemical groups in the graphene lattice was investigated by micro-XPS using an Escalab 250 Xi from Thermo. We were able to probe single isolated monolayers of mechanically exfoliated graphene using this technique. Extensive Raman measurements were then performed on pristine and modified mono- and bilayer graphene. Raman spectra were measured using a 100× objective at 514 nm on a Witec spectrometer. The laser power was adjusted to 0.7 mW and the spot size was about 1 μm.

3. Results and discussion

Attachment of foreign atoms to the graphene lattice was first confirmed using micro-XPS. Figure 1 shows carbon 1s spectra measured on pristine and plasma modified monolayer graphene flakes. The spectrum of pristine graphene presents a peak around 284.4 eV which is characteristic of sp^2 bonded carbon atoms. The red curve corresponds to the C 1s spectrum of the graphene after hydrogenation (120 s, 10 W, 0.1 Torr, position 1). We observe a small shoulder at higher binding energy, between 285 and 288 eV, which can be due to the incorporation of hydrogen (sp^3 C–H bonds appear around 285.0 eV) and a small amount of oxygen. The oxygen probably comes from the residual atmosphere that reacts with active sites and defects created by the plasma. In contrast, large changes are observed in the C 1s spectrum of fluorinated graphene (120 s, 10 W, 0.1 Torr, position 1): the main peak is shifted by ∼1 eV and new peaks arise at high binding energy. These peaks are attributed to carbon–fluorine bonds: C–CF, C–CF_2, C–F, CF–CF_n and CF_2 appear around 285.8 eV, 286.5 eV, 287.9 eV, 289.7 eV and 290.9 eV respectively (see curve fitting in figure 1(b)) [24]. The graphene C 1s spectrum after oxygen plasma looks similar but here the peaks at high binding energy are attributed to carbon–oxygen bonds. Figure 1(c) shows the peak fitting of the carbon 1s spectra of oxygen plasma treated graphene. The spectrum was decomposed into six components corresponding to sp^2 C–C, sp^3 C–C, hydroxyl, epoxy, carbonyl and carboxyl groups [24]. The relative concentration of these groups

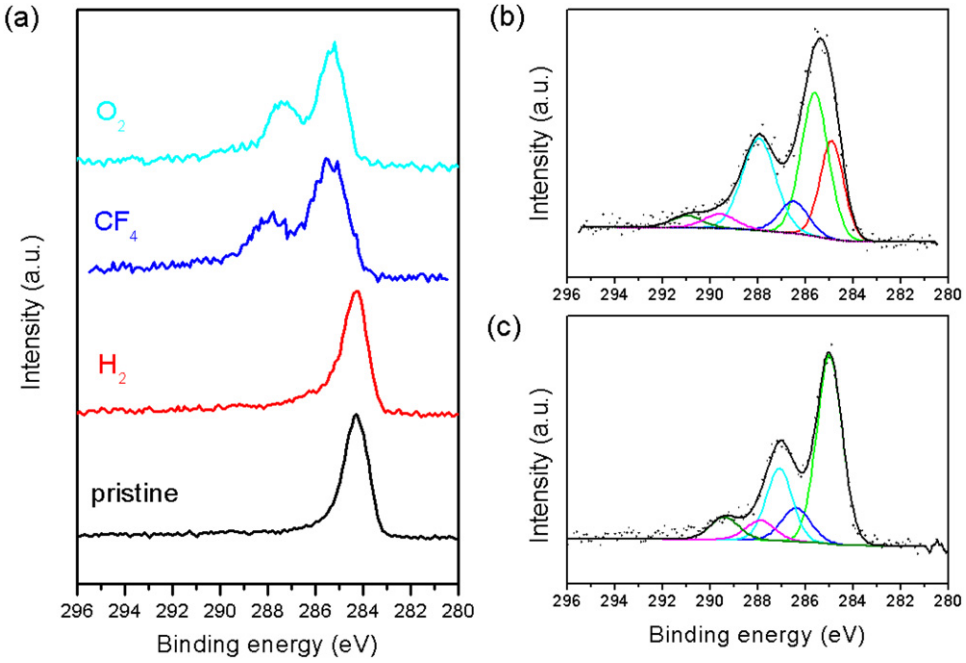

Figure 1. (a) Micro-XPS C 1s spectra of pristine, H_2 plasma, CF_4 plasma and O_2 plasma modified monolayer graphene. (b) Curve fitting of fluorinated graphene using six components: sp^3 C–C, C–CF, C–CF_2, C–F, CF–CF_n and CF_2. (c) Curve fitting of oxidized graphene using six components: sp^2 C–C, sp^3 C–C, hydroxyl, epoxy, carbonyl and carboxyl groups.

corresponds respectively to 0%, 52.3%, 10.6%, 22.2%, 6.4% and 8.5%. Using these values, we calculated an O/C ratio of 0.45. These numbers should be treated with care but nevertheless they reflect the chemical state of the surface, i.e. under these plasma conditions (O_2, 15 s, 10 W, 0.1 Torr, position 1) the sp^2 character of the graphene is completely lost and different oxygen groups including epoxy and carboxyl are grafted. As seen in figure 1(c), the most favorable configuration for oxygen atoms seems to be as epoxy groups. This is in agreement with experimental and theoretical studies which show that graphene functionalized using atomic oxygen results in epoxidation [6, 25]. Here, in addition to epoxy, other carbonyl and carboxyl groups are also grafted on the surface. These groups probably originate from the interaction of the graphene with various species from the plasma (presence of other species than atomic oxygen) and are usually observed after oxidative plasma treatment of graphene [26, 27]. In a previous work [5], we have shown that these groups could be used as an anchor point for further chemistry, which could be useful in applications such as chemical sensors or biosensors.

The XPS analysis of single graphene sheets thus shows that a large variety of functional groups can be attached to the graphene surface. Nevertheless we observe that plasma treatments can be sometimes too efficient: after only 15 s of oxygen exposure a very high content of oxygen is introduced in the carbon lattice leading to fast amorphization of graphene. In the following we will demonstrate that fine tuning of the functionalization strongly depends on the plasma parameters.

In this work, we used Raman spectroscopy as a fast, non destructive and powerful technique for the characterization of graphene [28], in particular for defect characterization [29–31]. The Raman spectra of monolayer graphene before and after oxygen plasma treatment are shown in figure 2. The pristine spectrum shows the two main peaks of graphene: the G band around 1580 cm^{-1} and the 2D band around 2700 cm^{-1} corresponding to the in-plane optical vibrational mode activated by an intervalley double resonance process [32]. After oxygen plasma exposure, new features corresponding to defect activated bands are appearing in the Raman spectra. The most prominent ones are the so called D and D′ band at ∼1340 cm^{-1} and ∼1620 cm^{-1} respectively.

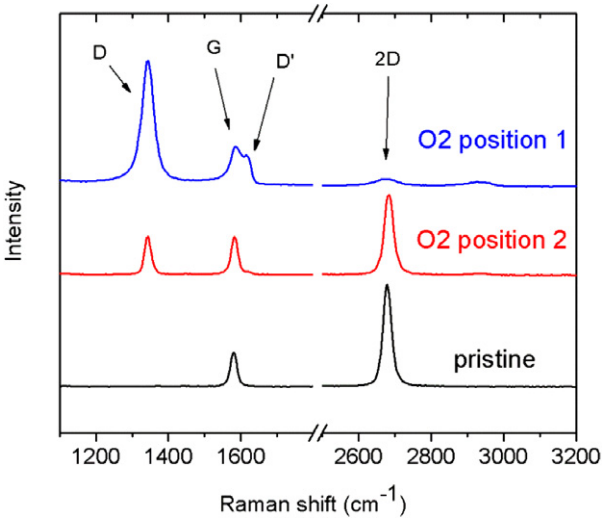

Figure 2. Raman spectra of oxygen plasma treated monolayer graphene under the following conditions: 10 W, 10 s, 0.1 Torr and inside the discharge (blue) or outside the discharge (red). The black curve shows Raman spectra of pristine graphene.

These defect activated peaks are particularly useful to monitor the structural changes induced in the graphene lattice. Indeed, the number of defects can be further quantified by using the integrated ratio of D and G band intensities, $I(D)/I(G)$. In the case of monolayer graphene, the $I(D)/I(G)$ curve exhibits two regions (see figure 4, red curve) [31, 33]. The first one (corresponding to short plasma-exposure time) is characterized by an increase of the $I(D)/I(G)$ ratio. This probably corresponds to the introduction of point defects into the sp^2 lattice where $I(D)/I(G) \sim 1/L_D^2$, with L_D the mean distance between two defects. The second region (corresponding to long plasma-exposure time) is characterized by a decrease in the intensity ratio due to a strong amorphization of the graphene produced by the high density of defects.

Recently, Cancado *et al* have proposed a relation valid for $L_D > 10$ nm, in order to calculate the average distance between defects in monolayer graphene [34],

$$L_D^2\ (\mathrm{nm}^2) = (1.8 \pm 0.5) \times 10^{-9}\ \lambda_L^4 \left(\frac{I_D}{I_G}\right)^{-1}$$

where λ_L is the wavelength of the laser, corresponding to 514 nm in our case. This equation was found for vacancies. However, we have recently showed that this can be extended to sp^3 defects [29]. If we now apply this equation to the red Raman spectrum in figure 2 (oxygen plasma treated graphene during 10 s outside the discharge), we obtain an L_D of $\sim$11.7 nm.

Finally, Raman spectroscopy can also be used to detect the nature of defects in graphene. Indeed, we recently showed that in the limit of low defect concentration, the intensity ratio between the D and D′ peaks is higher for sp^3 defects ($\sim$13) than for vacancies ($\sim$7) [29, 31]. In the case of our plasma treatments, we found that the $I(D)/I(D')$ is contained between 11 and 16 which confirms sp^3 modification.

3.1. Oxygen plasma. Effect of the position inside the chamber

The design of our plasma chamber allows us to position the sample in different regions. We investigated two different positions: one inside the discharge and the other outside the discharge (see section 2). This parameter is very important since the type and concentration of the reactive species, i.e. electrons, ions, radicals, strongly varies with the position: inside the discharge the excited species are more numerous and energetic while further away from it only long life time species such as radicals are present. Ions and electrons recombine quickly while metastable oxygen species can have radiative lifetimes of the order of seconds [35].

Figure 2 presents the Raman spectra of two graphene monolayers treated in both positions at the same time. After only 10 s of exposure inside the discharge, a large number of defects is introduced in the graphene lattice as can be seen by the large D peak, the mixing of the G and D′ peaks and the small 2D peak. This is typical of what has been reported in the literature. Nourbakhsh *et al* [6] obtained similar Raman spectra after exposure to oxygen plasma of 15 W for 3 s, while Gokus *et al* [22] after 1 s at 10 W. These results obviously depend on the plasma setup but nevertheless it is evident that under such severe conditions, i.e. sample inside the discharge, it is not possible to achieve fine modification of graphene because the process is too fast. Milder plasma conditions are thus necessary and can be obtained by moving the sample further away from the plasma discharge. The red curve in figure 2 shows the Raman spectrum of the monolayer graphene modified outside the discharge under the conditions previously used (10 W, 0.1 Torr, 10 s). We observe a relatively low intensity D peak, approximately the height of the G peak, and a very small D′ peak, which indicate that a very low number of defects are introduced in the graphene lattice. Indeed, by using the equation mentioned earlier we get a defect concentration of 1 for 1.7×10^4 carbon atoms. Away from the discharge, most energetic species have time to recombine avoiding fast etching of the graphene while interaction with atomic oxygen still allows chemical functionalization. Thus, by changing the sample position in the chamber, it is possible to slow down the oxidization process, allowing controllable modification of the graphene. Further discussion on oxygen plasma will thus proceed on samples treated in position 2.

3.2. Oxygen plasma. Effect of exposure time

Figure 3(a) shows the evolution of Raman spectra of graphene monolayer upon increasing oxygen plasma exposure outside the discharge region. We observe a smooth evolution of all features: the D peak is increasing slowly until 40 s and then decreasing; the D′ peak is appearing after 20 s, increases and merges with the G peak after 60 s; and the 2D peak decreases slowly to almost disappear after 120 s. A broadening of all peaks is also observed as the plasma duration is increasing. The slow and continuous evolution of the Raman spectra confirms that controlled modification of graphene by oxygen plasma is possible.

By using the $I(D)/I(G)$ ratio we found that L_D is 17.6, 11.7 and 8.2 nm for 5, 10 and 20 s oxygen plasma treatment, respectively. If we now assume that each defect contains one O atom we reach a C/O ratio of $\sim 35 \times 10^3$, $\sim 17 \times 10^3$ and $\sim 7 \times 10^3$, respectively. This result clearly shows that the number of functional groups can be finely tuned using remote oxygen plasma treatment.

3.3. Oxygen plasma. Mono versus bilayer graphene

Figure 3(b) shows the evolution of Raman spectra of bilayer graphene upon increasing oxygen plasma exposure. The plasma treatments were performed at the same position and simultaneously with the monolayer graphene samples displayed in figure 3(a). We can observe two main differences in the evolution of bilayer and monolayer graphene under oxygen plasma: (i) no defect peaks are observed at short plasma exposure (<20 s) and the height of the D peak is saturating after 60 s. The saturation is visible in figure 4 (black curve) where the ratio of the D and G peak areas, $A(D)/A(G)$, is plotted. We choose here to use the area ratio for the bilayer since its D peak cannot be fitted using one Lorentzian only, but

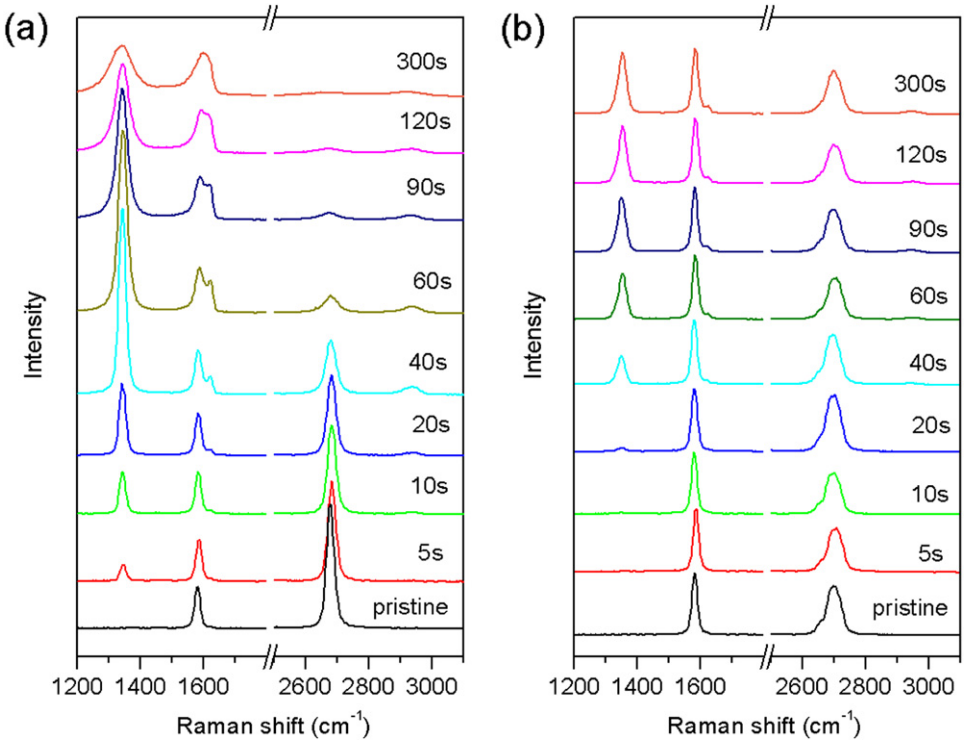

Figure 3. Evolution of Raman spectra of monolayer (a) and bilayer (b) graphene upon increasing oxygen plasma exposure outside the discharge region at position 2.

we need to use four components [32]. Thus, a bilayer is best characterized by the total peak area. For comparison purposes, $A(D)/A(G)$ is also plotted for the monolayer. $A(D)/A(G)$ reaches a maximum around 1 after 60 s for the bilayer while it rapidly increases to a maximum of 4.5 for the monolayer. The higher reactivity of monolayer graphene is usually attributed to its smaller intrinsic roughness [36] but a recent paper by Yamamoto *et al* [37] seemed to also incriminate charged impurities in the silicon oxide substrate. The presence of a plateau after 60 s of exposure tends to indicate that the bilayer graphene has reached a stable configuration where additional reactive species cannot attach to the surface. The oxygen species present in the post-discharge do not have enough energy to overcome the oxygenation barrier of the sp^2 carbons of the bilayer.

The absence of the D peak at short plasma exposure is further confirmed in figures 4(b) and (c) where Raman G and D peak maps of mono- and bilayer graphene after short plasma treatment are displayed. The bilayer is on the upper side and is attached to the monolayer. The D peak map shows that the monolayer has been homogeneously modified while the bilayer is intact. This difference could lead to a new way of performing fast and selective modification of monolayer graphene over bilayer using oxygen plasma.

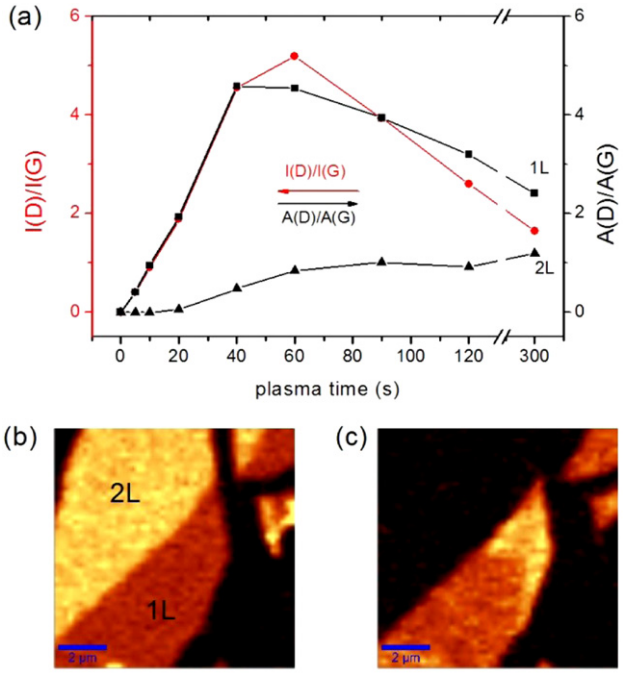

Figure 4. (a) $I(D)/I(G)$ and $A(D)/A(G)$ for mono- and bilayer graphene as a function of exposure time. (b) and (c) Raman maps of the G and D peak intensities for mono- and bilayer graphene after short oxygen plasma treatment.

3.4. Effect of the type of gas precursor. Tetrafluoromethane and hydrogen plasma

One of the main advantages of plasma treatment is that a large variety of gases can be used to modify the surface properties of materials. For example, if nitrogen containing groups are needed at the graphene surface, ammonia or nitrogen can be used as the feeding gas instead of oxygen [11, 12]. Here we compare hydrogenation and fluorination of mono-

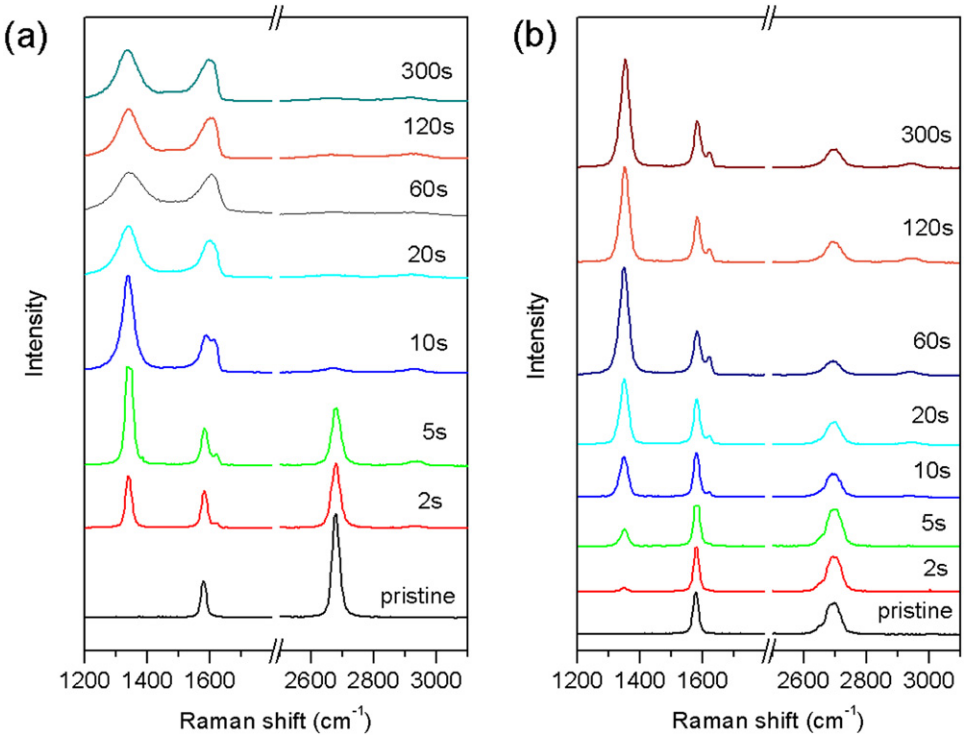

Figure 5. Evolution of Raman spectra of monolayer (a) and bilayer (b) graphene inside the discharge region at position 1 upon increasing CF_4 plasma exposure.

and bilayer graphene using H_2 and CF_4 gases. Fluorination of graphene is usually performed by exposure to F_2 gas under high temperature (400–600 °C) [38] or xenon difluoride (XeF_2) at room temperature [20, 19]. However, these methods are usually time consuming, poorly controllable and not compatible with SiO_2 supported graphene (F is known to etch Si). Recently SF_6 [15], CF_4 [13], Ar/F_2 [14] and CHF_3 [13] plasma were also applied on mono- and multilayer graphene, showing more controllable and faster modification.

Figure 5 shows the evolution of the Raman spectra of mono- and bilayer graphene upon increasing CF_4 plasma exposure. The samples were placed inside the discharge (position 1) since no modification occurred in the post-discharge even after 300 s. This absence of modification in position 2 could be due to lower density of fluorine radicals, shorter lifetime or smaller reactivity of the metastable species compared to those in oxygen plasma. We thus performed the fluorine attachment inside the plasma discharge (position 1). The modification of the monolayer graphene is fast and $I(D)/I(G)$ reaches a maximum between 5 and 10 s. At 10 s, the D′ peak merges with the G peak and the 2D band disappears. Interestingly, the Raman spectra do not change much after 60 s, which means that saturation coverage is reached. Furthermore, contrary to oxygen plasmas, no etching of the graphene occurs even for long exposure times. This confirms that F atoms do not chemically etch carbon and suggests that no ion bombardment of the sample is occurring. Indeed, CF_4 plasma is an electronegative media, which contains a large number of negative ions. In our experimental setup the sample is at floating potential and becomes negatively charged by the electrons from the plasma. Therefore, unlike positive ions, these negative ions are not accelerated towards the sample [39] and physical etching of the graphene is avoided.

If we now come back to the XPS C 1s spectrum of figure 1(b), we can estimate the F/C ratio after 120 s of treatment, i.e. at saturation coverage, using the area ratio of each component. We found that ∼31% of carbon atoms are bound to one fluorine atom which gives approximately $C_{3.2}F$. This value is in agreement (in the error limit of XPS peak fitting analysis) with the study by Robinson *et al* [20] where the authors experimentally found saturation coverage of one side fluorination of graphene by XeF_2 equal to C_4F. They further showed using density of states calculations that the C_4F configuration is the most energetically stable and that in this case the band gap of the material is expected to be 2.93 eV. The modification of graphene into an insulator with a large band gap after CF_4 plasma was confirmed by a large increase of the sheet resistivity (see figure S2 in SI available at stacks.iop.org/Nano/24/355705/mmedia). The XPS peak fitting of the carbon spectrum further shows that the majority of carbon–fluorine bonds are C–F (∼90%) with a smaller amount of $C–F_2$ (∼10%). These multiple fluorine bonds probably form at edges or defects.

As observed in oxygen plasma, fluorination is more favorable for monolayer than for bilayer graphene. The D and D′ peaks in the bilayer spectra slowly increase until they reach a maximum after 60 s (see figure 5(b)). After that no change in the Raman spectra occurs. This result differs from SF_6 [15] and Ar/F_2 [14] plasma where only a small D peak is observed in the bilayer. This could be explained by the presence of more energetic or higher density of species in our CF_4 plasma

due to the different plasma system and conditions used. Such an example shows again the complexity of a plasma gas and the difficulty obtaining similar results going from one experimental setup to another.

Finally hydrogen plasma treatment was also performed on mono- and bilayer graphene. The same plasma parameters were used, i.e. 0.1 Torr, 10 W, and inside the discharge region at position 1. The defect density (A(D)/A(G)) induced on the mono- and bilayer is displayed in figure 6 (see figure S3 in SI for full Raman spectra available at stacks.iop.org/Nano/24/355705/mmedia). Hydrogenation is more controllable than fluorination and reaches a maximum defect density after 60 s of exposure. Surprisingly however, similar hydrogenation rates are obtained for mono- and bilayer graphene, which indicates a different reaction mechanism compared to the O_2 and CF_4 plasmas. This difference could be due to the presence of more energetic species reaching the graphene surface. If we look in the literature two types of graphene hydrogenation have been reported. The first one, which usually requires long exposure time, involves atomic hydrogen radicals and is performed outside the discharge [40, 18]. These radicals have low energy and are able to modify only the more reactive parts of the monolayer (defects or ripples): the adsorption energy barrier for hydrogen bonding is lower in regions where the sp^2 lattice exhibits curvature [41] (an atomic level), which induces differences in the modification of the corrugated monolayer and the smoother bilayer graphene. Charged inhomogeneity in the substrate could also be an explanation for enhanced monolayer reactivity [37]. In the second type of hydrogenation, the graphene samples are directly immersed inside the plasma [7–9]. In this case, the graphene is exposed to atomic hydrogen but also to other more energetic species such as H^+ and H_3^+ ions. These positive ions can be accelerated towards the graphene and acquire enough energy to overcome the hydrogenation barrier for both mono- and bilayer graphene, leading to a similar modification rate. In order to fully understand the role of ions and radicals in the hydrogenation of graphene, further measurements of the plasma characteristics using tools such as optical emission spectroscopy, Langmuir probe and mass spectrometry would be useful.

In figure 6, we further observe that the A(D)/A(G) ratio for the monolayer and bilayer is mostly similar except at 300 s where it is smaller for the bilayer. This difference at long exposure time could be attributed to the layer-by-layer modification of the graphene by plasma treatments, i.e. in a bilayer graphene the top layer is first modified and the bottom layer starts to react only when the first layer is etched away. After 300 s of H_2 plasma, we observe that the monolayer graphene is highly modified: large D peak, mixing of G and D′ peaks and small 2D peak (see figure S3 in SI available at stacks.iop.org/Nano/24/355705/mmedia). If the modification rates of the bilayer and monolayer are similar, as we noticed for hydrogen plasma, after 300 s of treatment the top layer of the bilayer should be completely modified while the bottom layer should stay mostly unaffected. This is showing up in the A(D)/A(G) ratio: the G peak intensity of the bottom layer stands out giving a smaller value compared to the monolayer.

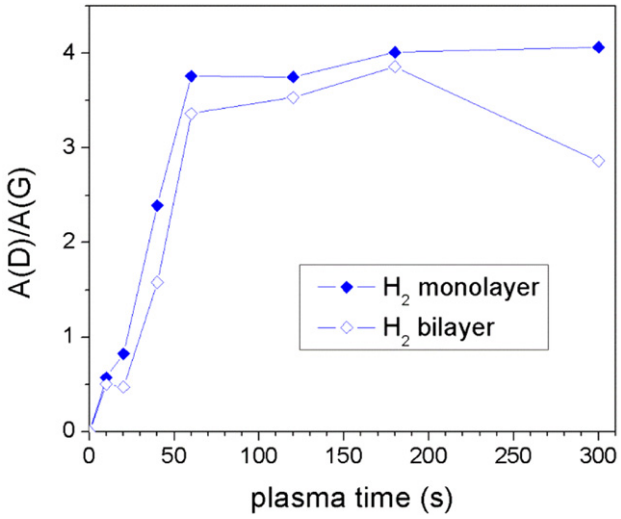

Figure 6. A(D)/A(G) for mono- and bilayer graphene treated using H_2 plasma inside the discharge region at position 1 as a function of exposure time.

4. Conclusions

In this work, we have shown highly controllable modification of mono- and bilayer graphene using oxygen, hydrogen and tetrafluoromethane plasma treatments. All treatments were performed in the same setup to allow comparison of the results. We found that depending on the plasma parameters such as exposure time and sample position inside the chamber, fine tuning of the functionalization can be obtained for all types of plasmas. Hydrogen, oxygen and fluorine containing groups were successfully grafted on the graphene. Using micro-XPS we showed that the fluorine saturation coverage was close to C_4F with predominant single C–F bonds, in agreement with previous studies. At this fluorine coverage the graphene becomes a large band gap insulator as indicated by its increased resistivity. By positioning the sample outside the oxygen plasma discharge we obtained very fine tuning of the defect density. The average distance between defects, calculated by Raman spectroscopy, could be brought up to ∼17 nm, i.e. one defect for 3.5×10^4 carbon atoms. Moreover we showed selective oxygen functionalization of monolayer over bilayer graphene at short exposure time. Lower reactivity of the bilayer graphene was found for O_2 and CF_4 plasma but this distinction is not observed in the case of hydrogenation. We attribute this difference to the presence of more energetic species in the hydrogen plasma such as positive ions that could play an important role in the functionalization process. Our results show that plasma treatment is a useful and versatile tool, which could be easily implemented in several graphene applications that require control of doping or resistivity, opening of band gap or simply presence of functional groups.

Acknowledgments

AF and CC acknowledge the Alexander von Humboldt foundation for financial support. AF acknowledges the FRS-FNRS for financial support.

References

[1] Geim A K 2009 Graphene: status and prospects *Science* **324** 1530–4

[2] Geim A K and Novoselov K S 2007 The rise of graphene *Nature Mater.* **6** 183–91

[3] Novoselov K S, Fal'ko V I, Colombo L, Gellert P R, Schwab M G and Kim K 2012 A roadmap for graphene *Nature* **490** 192–200

[4] Peltekis N, Kumar S, McEvoy N, Lee K, Weidlich A and Duesberg G S 2012 The effect of downstream plasma treatments on graphene surfaces *Carbon* **50** 395–403

[5] Felten A, Flavel B S, Britnell L, Eckmann A, Louette P, Pireaux J J, Hirtz M, Krupke R and Casiraghi C 2013 Single- and double-sided chemical functionalization of bilayer graphene *Small* **9** 631–9

[6] Nourbakhsh A, Cantoro M, Vosch T, Pourtois G, Clemente F, van der Veen M H, Hofkens J, Heyns M M, De Gendt S and Sels B F 2010 Bandgap opening in oxygen plasma-treated graphene *Nanotechnology* **21** 435203

[7] Wojtaszek M, Tombros N, Caretta A, van Loosdrecht P H M and van Wees B J 2011 A road to hydrogenating graphene by a reactive ion etching plasma *J. Appl. Phys.* **110** 063715

[8] Luo Z, Yu T, Kim K-J, Ni Z, You Y, Lim S, Shen Z, Wang S and Lin J 2009 Thickness-dependent reversible hydrogenation of graphene layers *ACS Nano* **3** 1781–8

[9] Jaiswal M, Haley C, Xuan Y, Bao Q, Toh C T and Loh K P 2011 Controlled hydrogenation of graphene sheets and nanoribbons *ACS Nano* **5** 888–96

[10] Jung R and Cheong J-K 2012 Investigation of the dependence of the chemical states of the graphene surface on N_2 plasma treatment *J. Korean Phys. Soc.* **60** 933–6

[11] Lin Y-C, Lin C-Y and Chiu P-W 2010 Controllable graphene N-doping with ammonia plasma *Appl. Phys. Lett.* **96** 133110

[12] Baraket M, Stine R, Lee W K, Robinson J T, Tamanaha C R, Sheehan P E and Walton S G 2012 Aminated graphene for DNA attachment produced via plasma functionalization *Appl. Phys. Lett.* **100** 233123

[13] Chen M, Zhou H, Qiu C, Yang H, Yu F and Sun L 2012 Layer-dependent fluorination and doping of graphene via plasma treatment *Nanotechnology* **23** 115706

[14] Tahara K, Iwasaki T, Matsutani A and Hatano M 2012 Effect of radical fluorination on mono- and bi-layer graphene in Ar/F_2 plasma *Appl. Phys. Lett.* **101** 163105

[15] Yang H, Chen M, Zhou H, Qiu C, Hu L, Yu F, Chu W, Sun S and Sun L 2011 Preferential and reversible fluorination of monolayer graphene *J. Phys. Chem.* C **115** 16844–8

[16] Wu J, Xie L, Li Y, Wang H, Ouyang Y, Guo J and Dai H 2011 Controlled chlorine plasma reaction for noninvasive graphene doping *J. Am. Chem. Soc.* **133** 19668–71

[17] Tang Y, Yin L, Yang Y, Bo X, Cao Y, Wang H and Zhang W 2012 Tunable band gaps and p-type transport properties of boron-doped graphenes by controllable ion doping *ACS Nano* **6** 1970–8

[18] Elias D C *et al* 2009 Control of graphene's properties by reversible hydrogenation: evidence for graphane *Science* **323** 610–3

[19] Nair R R *et al* 2010 Fluorographene: a two-dimensional counterpart of Teflon *Small* **6** 2877–84

[20] Robinson J T *et al* 2010 Properties of fluorinated graphene films *Nano Lett.* **10** 3001–5

[21] Boukhvalov D and Katsnelson M 2008 Tuning the gap in bilayer graphene using chemical functionalization: density functional calculations *Phys. Rev.* B **78** 1–5

[22] Gokus T, Nair R R, Bonetti A, Böhmler M, Lombardo A, Novoselov K S, Geim A K, Ferrari A C and Hartschuh A 2009 Making graphene luminescent by oxygen plasma treatment *ACS Nano* **3** 3963–8

[23] Felten A, Bittencourt C, Pireaux J J, Van Lier G and Charlier J C 2005 Radio-frequency plasma functionalization of carbon nanotubes surface O_2, NH_3, and CF_4 treatments *J. Appl. Phys.* **98** 074308

[24] Beamson G and Briggs D 1992 *High Resolution XPS of Organic Polymers* (New York: Wiley)

[25] Johns J E and Hersam M C 2013 Atomic covalent functionalization of graphene *Acc. Chem. Res.* **46** 77–86

[26] McEvoy N, Nolan H, Ashok Kumar N, Hallam T and Duesberg G S 2013 Functionalisation of graphene surfaces with downstream plasma treatments *Carbon* **54** 283–90

[27] Liu L, Xie D, Wu M, Yang X, Xu Z, Wang W, Bai X and Wang E 2012 Controlled oxidative functionalization of monolayer graphene by water-vapor plasma etching *Carbon* **50** 3039–44

[28] Casiraghi C 2012 Raman spectroscopy of graphene *Spectroscopic Properties of Inorganic and Organometallic Compounds: Techniques Materials and Applications* (Cambridge: RSC) pp 29–56

[29] Eckmann A, Felten A, Verzhbitskiy I, Davey R and Casiraghi C A 2013 multi-wavelenght Raman study on the nature of defects in graphene *Phys. Rev.* B **88** 035426

[30] Casiraghi C 2009 Probing disorder and charged impurities in graphene by Raman spectroscopy *Phys. Status Solidi-Rapid Res. Lett.* **3** 175–7

[31] Eckmann A, Felten A, Mishchenko A, Britnell L, Krupke R, Novoselov K S and Casiraghi C 2012 Probing the nature of defects in graphene by Raman spectroscopy *Nano Lett.* **12** 3925–30

[32] Ferrari A C 2007 Raman spectroscopy of graphene and graphite: disorder, electron–phonon coupling, doping and nonadiabatic effects *Solid State Commun.* **143** 47–57

[33] Lucchese M M, Stavale F, Ferreira E H M, Vilani C, Moutinho M V O, Capaz R B, Achete C A and Jorio A 2010 Quantifying ion-induced defects and Raman relaxation length in graphene *Carbon* **48** 1592–7

[34] Cançado L G, Jorio A, Ferreira E H M, Stavale F, Achete C A, Capaz R B, Moutinho M V O, Lombardo A, Kulmala T S and Ferrari A C 2011 Quantifying defects in graphene via Raman spectroscopy at different excitation energies *Nano Lett.* **11** 3190–6

[35] Fridman A and Kennedy L A 2004 *Plasma Physics and Engineering* (London: Taylor and Francis)

[36] Meyer J C, Geim A K, Katsnelson M I, Novoselov K S, Booth T J and Roth S 2007 The structure of suspended graphene sheets *Nature* **446** 60–3

[37] Yamamoto M, Einstein T L, Fuhrer M S and Cullen W G 2012 Charge inhomogeneity determines oxidative reactivity of graphene on substrates *ACS Nano* **6** 8335–41

[38] Withers F, Russo S, Dubois M and Craciun M F 2011 Tuning the electronic transport properties of graphene through functionalisation with fluorine *Nanoscale Res. Lett.* **6** 526

[39] Stoffels E, Stoffels W W and Kroesen G M W 2001 Plasma chemistry and surface processes of negative ions *Plasma Sources Sci. Technol.* **10** 311–7

[40] Diankov G, Neumann M and Goldhaber-Gordon D 2013 Extreme monolayer-selectivity of hydrogen-plasma reactions with graphene *ACS Nano* **7** 1324–32

[41] Ruffieux P, Gröning O, Bielmann M, Mauron P, Schlapbach L and Gröning P 2002 Hydrogen adsorption on sp^2-bonded carbon: influence of the local curvature *Phys. Rev.* B **66** 245416